Journal of Bioprocessing & Biotechniques

Almeida et al., J Bioprocess Biotech 2016, 6:3
http://dx.doi.org/10.4172/2155-9821.1000272

Research Article Open Access

Ultra-Thin Films of Reduced Graphene Oxide (RGO) Nanoplatelets Functionalized with Different Organic Materials

Tiago P Almeida[1,2], Celina M Miyazaki[3], Diogo Volpati[4], Tatiana A Silva[5], Maria Luisa Braunger[5], Anerise de Barros[6], Frank Hollmann[2] and Antonio Riul Jr[1,5]*

[1]*PIPG Bioenergia-UNICAMP, Campinas, SP, Brazil*
[2]*Department of Biotechnology, Delft University of Technology, Delft, The Netherlands*
[3]*Centro de Ciências e Tecnologias para a Sustentabilidade- UFSCa, Sorocaba, SP, Brazil*
[4]*Department of Natural Sciences, Mid Sweden University, SE-851 70, Sundsvall, Sweden*
[5]*Applied Physics Department, "Gleb Wataghin" Institute of Physics, University of Campinas (UNICAMP), SP, Brazil*
[6]*Functional Materials Laboratory, Institute of Chemistry, University of Campinas (UNICAMP), SP, Brazil*

Abstract

This work aims the functionalization of reduced graphene oxide nanoplatelets with chitosan (G-chitosan) and also with poly(styrenesulfonic acid) (GPSS), thus forming stable, dispersed aqueous solutions. G-chitosan and GPSS solutions allowed the layer-by-layer (LbL) film formation with glucose oxidase (GOx), establishing multilayered nanostructures with elevated control in thickness and morphology. The graphene nanoplatelets were characterized by UV-vis and FTIR spectroscopies, resulting in good adherence and linear deposition of the graphene nanoplatelets with GOx in the LbL structures. Cyclic voltammetry shows an enlargement in the current intensity with increasing number of deposited LbL layers, possibly owing to the formation of conducting paths by the graphene nanoplatelets in the tailored multilayer nanomaterial formed.

Keywords: Glucose oxidase; Graphene nanoplatelets; Layer-by-layer films

Abbreviations: LbL: Layer-by-Layer; GOx: Glucose Oxidase; G-chitosan: Reduced Graphene Oxide Nanoplatelets Functionalized with Chitosan; GPSS: Reduced Graphene Oxide Nanoplatelets Functionalized with Poly(Styrenesulfonic Acid).

Introduction

Graphene is a hexagonal mesh of carbon atoms bonded in a hexagonal sp^2 array, in this work produced by the Hummers method [1,2]. Briefly, Graphene Oxide (GO) is a common precursor from the chemical exfoliation method [2] being electrically insulating [3]. It is an atomically thin sheet of graphite covalently linked to oxygenated functional groups on the basal plane and at the edges, containing a mixture of sp^2 and sp^3 carbon atoms. The reduced form of graphene oxide (rGO) studied in this paper has low oxygenated functional groups content and exhibits electric and mechanical properties similar to pristine graphene [4].

Despite of being applied in a plethora of applications [5], it has been an issue to cover large areas with pristine graphene and an alternative is the use of nanolayered structures. In this paper we employed the Layer-by-Layer (LbL) technique to build up a laminated interlocked structure of the rGO nanoplatelets with Glucose Oxidase (GOx). The LbL method allows a simple, fast, versatile and reproducible way to modify large areas with good control over thickness and morphology of the film. It has been successfully applied to form ultrathin films of graphene and carbon nanotubes [6-9], enabling similarly, the immobilization of enzymes in highly-ordered nanostructures [10,11]. The presence of graphene nanoplatelets dispersed in multilayered LbL architectures might bridge a favorable charge transfer path from the immobilized enzyme to the electrode, paving the way for future applications as biofuel cell and biosensors. The multilayered film reported here can be favorably used at the electrode interface with biological materials as an easy approach to sequestrate electrons in biosensing and biofuel cell developments.

In this work, rGO nanoplatelets were combined with poly(styrenesulfonic acid) (GPSS) and chitosan (G-chitosan) in order to produce water soluble and electrically charged materials, enabling the film grown by the LbL deposition. The materials were characterized by ultraviolet-visible (UV-vis) and Fourier transform infrared (FTIR) spectroscopies, indicating an effective reduction process to form reduced graphene nanoplatelets. LbL films were easily assembled using GPSS and G-chitosan with GOx, further characterized by cyclic voltammetry, which pointed out an increase in the current intensities due to the presence of graphene nanoplatelets in the film nanostructure.

Materials and Methods

Materials

Graphite powder (98%) from Synth, potassium permanganate ($KMnO_4$, 99%), sulfuric acid (H_2SO_4, 97%) and potassium thiosulfate ($K_2S_2O_3$, 99%) from Ecibra, hydrogen peroxide (H_2O_2, 30%), hydrazine sulfate ($H_6N_2O_4S$) and phosphorous pentoxide (P_2O_5) from Vetec, glucose oxidase (from *Aspergillus niger*) (GOx) (type VII, lyophilized powder, ≥ 100,000 units/g solid, without added oxygen) and poly(sodium 4-styrenesulfonate) (PSS) (M_w 70,000) from Sigma-Aldrich were all used as received. Chitosan was obtained from shrimp shells using the method described by Bought et al. resulting in a material with molecular weight $M_w=9 \times 10^4$ g.mol^{-1} with acetylation degree 14 [12].

***Corresponding author:** Antonio Riul Jr., Applied Physics Department, "Gleb Wataghin" Institute of Physics, University of Campinas (UNICAMP), SP, Brazil, Tel: 551-935-215-336; E-mail: ariuljr@gmail.com

Received March 03, 2016; **Accepted** March 18, 2016; **Published** March 22, 2016

Citation: Almeida TP, Miyazaki CM, Volpati D, Silva TA, Braunger ML, et al. (2016) Ultra-Thin Films of Reduced Graphene Oxide (RGO) Nanoplatelets Functionalized with Different Organic Materials. J Bioprocess Biotech 6: 272. doi:10.4172/2155-9821.1000272

Procedures

Initially, Graphene Oxide (GO) was obtained from the Hummers' method [2,13], 0.1 g of GO was solubilized in water (50 mL) and sonicated for 600 s. 250 mg of chitosan was solubilized in 50 mL of HCl 0.05 mol.L^{-1} and similarly sonicated for 600 s. After that both solutions were mixed with 0.1302 g of $H_6N_2O_4S$ (hydrazine) in order to start the reduction and functionalization processes, stirred at 70°C under reflux for 20 hours. The final product consists in rGO nanoplatelets functionalized with chitosan (G-chitosan). A similar process was applied to obtain reduced graphene oxide functionalized with PSS (GPSS). To this end, 0.5 g of GO were sonicated in 50 mL of water for 600 s. Then, 0.5 g of PSS and 0.0651 g of hydrazine were added, with the final solution stirred at 90°C for 12 hours under reflux.

LbL films fabrication

Instead of using the traditional dipping method [8], we applied small drops of the polyelectrolytes to cover the surface of carbon Screen-Printed Electrode (SPE), as described below. Briefly, a drop of G-chitosan was kept 15 min onto the SPE, followed by a washing step to remove molecules loosely bound to the electrode surface. Then a drop of GPSS (oppositely charged material) was sequentially spread and kept 15 min onto the SPE/G-chitosan interface, thus forming a bilayer $(G\text{-chitosan/GPSS})_1$. The process is repeated until the formation of five bilayers $(G\text{-chitosan/GPSS})_5$ onto the SPE, with a final GOx layer deposited onto it. GPSS, GOx and G-chitosan solutions were all at 1.0 mg.mL^{-1} suspended in 0.1 mol.L^{-1} phosphate buffer salt (PBS) solution (pH 6.2).

Casting films fabrication

For the FTIR analysis casting films were formed onto silicone substrates from concentrated solutions of the polyelectrolytes.

Instrumentation

All solutions were prepared with ultrapure water acquired from a Sartorius system, model Arium Comfort. The solutions were also briefly sonicated using a probe from QSonica Sonicators, model Q700. UV-Vis (Biochrom Libra S60 spectrophotometer) and FTIR (Thermo Nicolet spectrometer, model Nexus 470 in transmission) spectroscopies were used to confirm the effectiveness of the rGO synthesis and functionalization. The performance of the LbL films composed by GOx, G-chitosan and GPSS was evaluated using cyclic voltammetry (Autolab Potentiostat/Galvanostat, model PGSTAT302N). All LbL films were deposited onto carbon screen-printed electrodes (SPE DropSens 110, commercially obtained from Methron) as described previously, with electrochemical measurements taken at a scan rate potential of 80 mV.s^{-1}.

Results and Discussion

The UV-vis absorbance spectra for GO, chitosan and G-chitosan are illustrated in Figure 1a, while those for PSS and GPSS solutions are illustrated in Figure 1b, confirming the successful synthesis and functionalization processes. All the spectra were normalized to remove concentration effects over the samples analyzed, focusing mainly on the peak positions. It is possible to observe two characteristics bands for GO, one at 232 nm characteristic of $\pi \rightarrow \pi^*$ transition in aromatic C-C bonds, and other at 302 nm assigned to $n \rightarrow \pi^*$ transition in C=O binding [14]. When GO is functionalized with PSS or chitosan it is possible to note a redshift in the $\pi \rightarrow \pi^*$ transition band. The band at 232 nm from GO shifts to 271 nm in GPSS and to 263 nm in G-chitosan, clearly indicating the electronic conjugation reestablishment after the reduction and functionalization processes [14,15]. In the GPSS spectrum it is also remarkable the presence of a band at 225 nm, corresponding to the absorption of the PSS benzene group [16], easily compared to the pristine PSS spectra. It was also observed a band at 197 nm in the chitosan spectrum, from N-acetyl-glucosamine (GlcNAc) and glucosamine (GlcN) chromophoric groups [17].

From the solutions of G-chitosan and GPSS, LbL films were grown using GOx as a counter-solution required for the electrostatic interactions governing the film grown. The adsorption kinetics of the LbL films is illustrated in Figure 2. In short, the LbL film formation was monitored at each deposition step, fixing the GOx deposition time at 180s, with a varying immersion time deposition for G-chitosan (Figure 2a). A plot of the cumulative G-chitosan time (Figure 2b) clearly indicates a plateau after 900 s, indicative that no effective material adsorption occurs after that. The same procedure was repeated fixing the G-chitosan deposition time at 900 s, now varying the GOx immersion time (results not shown). Similarly, the best deposition time for G-chitosan was obtained at ~ 900 s (results not show). It was observed a linear dependence (Figure 2c) in the LbL film growth using the optimized deposition times, revealing that the similar amount of material is being transferred at each deposition step in the

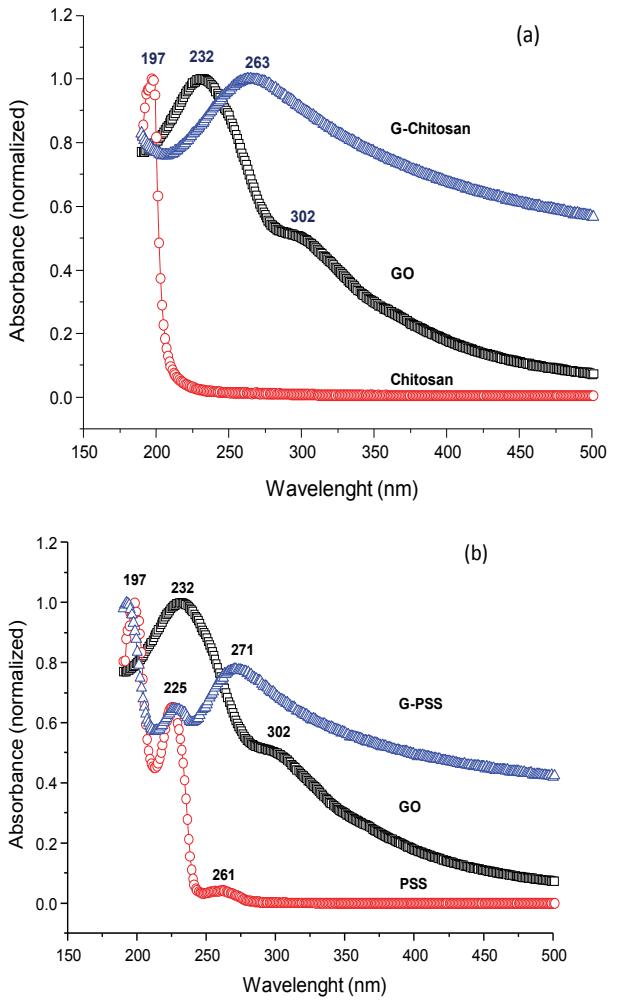

Figure 1: UV-Vis absorbance spectra of solutions prepared in ultrapure water: (a) GO, chitosan and G-chitosan and (b) GO, PSS and GPSS.

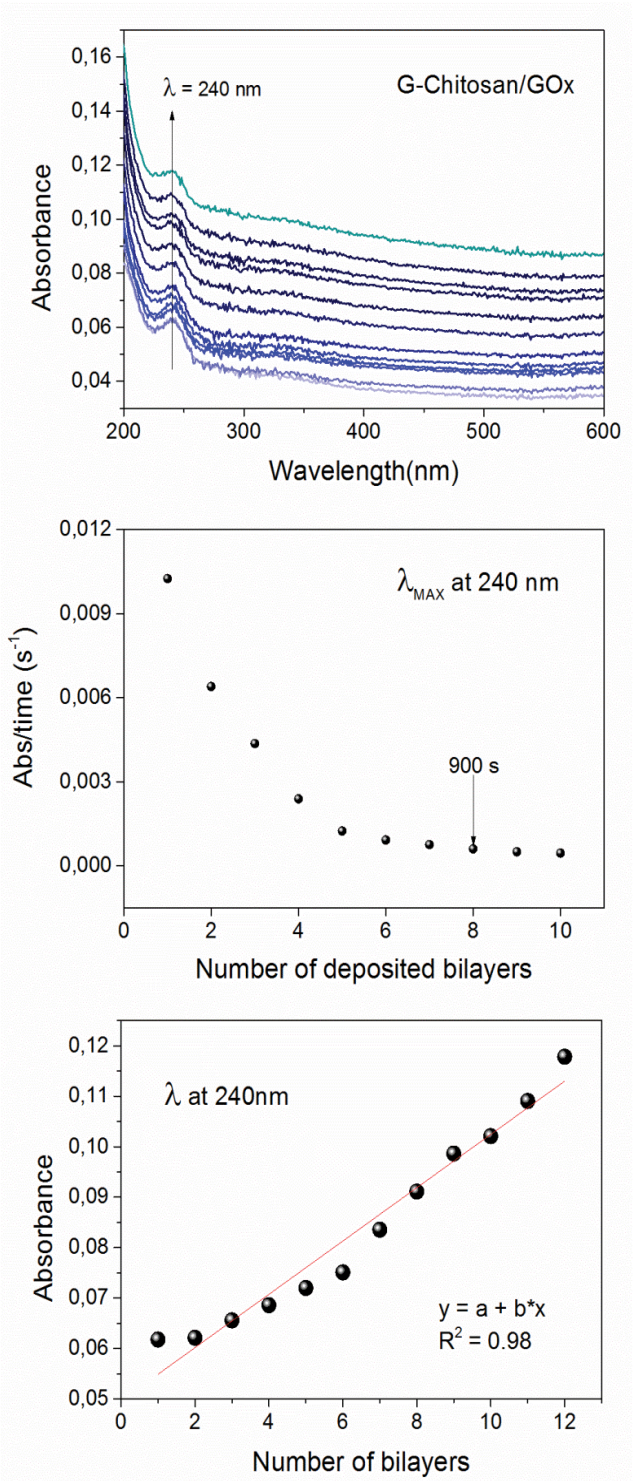

Figure 2: (a) UV absorbance for the LbL assembly. Black arrow indicates increasing absorbance at 240 nm with the number of deposited layers; (b) kinetic growth plot used to choose the best deposition time; (c) linear dependence of absorbance (λ_{max}=225 nm) at each deposition step for the (G-chitosan/GPSS/GOx) LbL film. No significant changes in absorbance are observed after 900 s.

nanostructures formed [18]. Likewise, the best deposition time for GPSS was achieve at 300 s (results not shown), but we decided to use 900 s just to keep the same time immersion in the LbL setup.

To investigate the intermolecular interactions governing the functionalization, the FTIR spectra for GO, chitosan, G-chitosan, PSS and GPSS (presented in the Figures 3a and 3b), confirmed interactions between materials and effectiveness of the reduction process adopted. However, the nature of those interactions is different for both G-Chitosan and GPSS. Common for both materials the FTIR spectrum of GO nanoplatelets shows strong characteristic peaks at 1735 cm^{-1} (C=O carbonyl stretching), 1602 cm^{-1} (sp^2-hybridized C=C in plane vibrations), 1423 cm^{-1} (OH deformation of the C-OH groups), 1219 cm^{-1} (C-OH stretching vibration) and 1045 cm^{-1} (C-O stretching vibrations) [19,20], which can be the basis for our interaction investigations. In Figure 3a, two characteristic peaks were slightly shifted in the G-chitosan spectrum when compared to pristine chitosan and GO. The main observed changes were from 1735 to 1717 cm^{-1} (C=O carbonyl stretching vibrations assigned to GO) and other from 1089 to 1100 cm^{-1} (C-O stretching glucoside ring assigned to chitosan) [21,22], with wavenumbers highlighted in Figure 3a. A third peak could also be a shift from 1508 (chitosan) or 1427 (GO) to 1451 cm^{-1} (G-Chitosan), probably due to the interaction between chitosan and the formed rGO nanoplatelets [21,22]. However, the uncertainty about this broad peak hampers its assignment, but it does not pledge the conclusions about a chemical interaction between the GO and the chitosan. On the other hand, it was noticed physical interaction (van der Waals) between PSS and rGO nanoplatelets since no new bands or peak shifts were observed in the GPSS spectrum compared with the neat materials spectra; the GPSS spectrum can be called a sum of the bands observed at the PSS and rGO spectra. Very small shifts were observed, for instance from 1128 to 1132 cm^{-1} possibly due to hydrophobic interactions between the sp^2 network in the nanoplatelets with the benzene ring in PSS [23]. No conclusions can be drawn in this region since it is inside the equipment error (4 cm^{-1}), reinforcing the physical interaction nature of these interactions. It is important to mention that the region of C-H, N-H and O-H stretching (from 2800 up to 3700 cm^{-1}) were also analyzed, but no relevant results were obtained due to the low signal-to-noise ratio (results not shown). These findings are in good agreement with the reestablishment of the sp^2 conjugation presented in Figure 2, followed by an effective functionalization of the rGO nanoplatelets with chitosan (G-chitosan) and PSS (GPSS) during the synthesis. The main FTIR peak assignments for GO, chitosan and PSS are displayed in Table 1.

The linear electrochemical response in Figure 4 indicates the presence of a diffusive process controlled by the surface of the LbL modified electrodes. The absence of redox peaks in the CV experiments point out to a possible strong electrochemical double-layer effect governing the system [24,25]. In addition, higher current values were observed for the LbL films when compared with bare SPE electrodes analyzing the currents as a function of the scanning rate in the 20-100 $mV.s^{-1}$ intervals. Each curve displayed in Figure 4 presented good stabilization after 3 scan cycles, a significant capacitive behavior due to the presence of graphene nanoplatelets. The flat oxidative performance in the voltammograms imply in a lower resistance of the system to release storage charges due to the presence of the rGO nanoplatelets, which also promotes a better electron transfer between the LbL modified electrode and the buffer solution.

The anodic peak current exhibited a linear relationship with the number of deposited bilayers (Figure 5), displaying once again good capacitance contribution from the rGO nanoflakes. The linearity observed in Figure 5B points out to equal changes in the measured current as the film thickness increases, possibly due to the same amount of material transferred at each LbL step deposition, corroborating

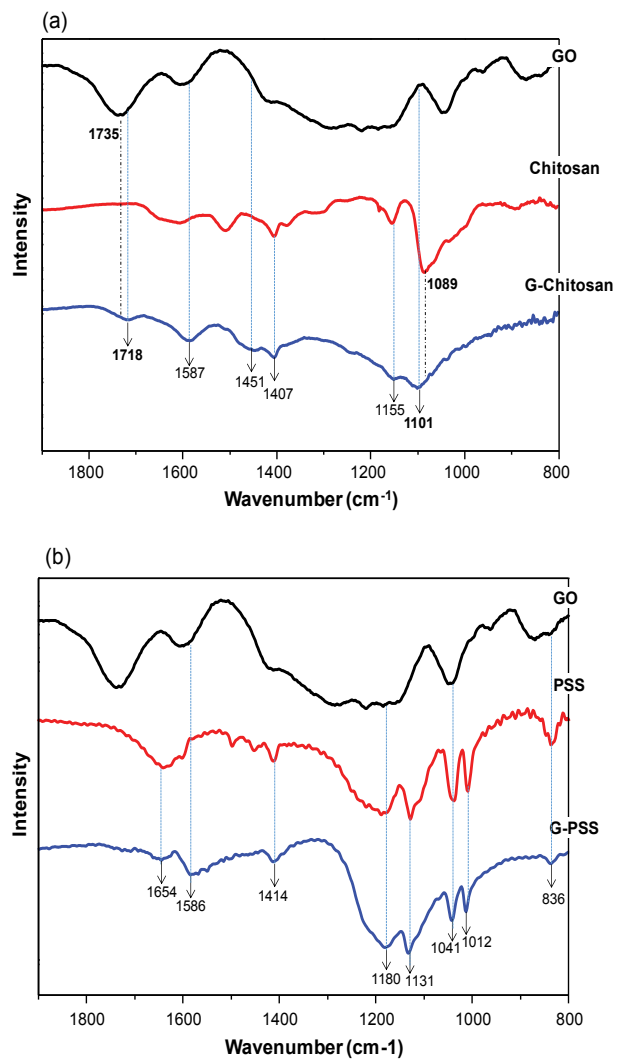

Figure 3: FTIR spectra in transmission mode for: (a) GO, chitosan and G-chitosan; (b) GO, PSS and GPSS.

GO		Chitosan		PSS	
Wavenumber (cm^{-1})	Assignment	Wavenumber (cm^{-1})	Assignment	Wavenumber (cm^{-1})	Assignment
1733	v C=O	~1655	v C=O	1633	v C=C
1610	v_{as} COO^-	1510	δ $-NH_3^+$	1598	C=C
1427	v_s COO^-	1409	δ O−H/C−H	1498	v C=C
1222	v C=O	1155	C−O−C	1452	C=C
1045	v C−O	1089	v CO	1180	v_{as} S=O
				1128	ring
				1041	v_s S=O
				1006	δ ring

Table 1: FTIR peaks positions and assignments [19-22,24] for GO, chitosan and PSS films. In the table, the molecules vibrations are abbreviated using v: stretching; v_{as}: asymmetric stretching; v_s: symmetric stretching; δ: deformation.

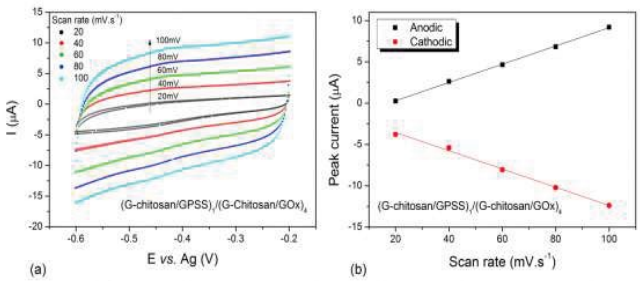

Figure 4: (a) Cyclic voltammetry at different scan rates; (b) Peak current vs. scan rate for $(G\text{-chitosan/GPSS})_1/(G\text{-chitosan/GOx})_4$ LbL film immersed in 0.1 M PBS and pH 6.2.

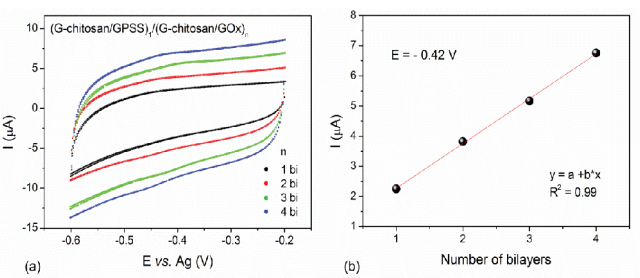

Figure 5: (a) Cyclic voltammograms conducted at 80 $mV.s^{-1}$ scan rate for 1, 2, 3 and 4 bilayers and (b) plot of the anodic peak vs. number of bilayers for $(G\text{-chitosan/GPSS})_1/(G\text{-chitosan/GOx})_4$ immersed in aqueous 0.1M PBS pH 6.2.

results presented in Figure 2. Here, the identical changes in current can be attributed to effective laminated interlocked conductive paths formed by the graphene nanoplatelets in the LbL film structure with the electrode surface, without noticeable effects from the wrapping materials (chitosan or PSS).

Conclusions

The reduction process was efficient to create rGO nanoplatelets dispersed with chitosan or PSS. The spectroscopic characterization indicated good reestablishment of the sp^2 hybridization in the formed nanoplatelets, pointing out to a chemical interaction between chitosan and rGO, and a physical interaction between PSS and the nanoplatelets. A linear transfer of the materials was observed in the LbL film formation, showing that similar amounts of material being transferred at each deposition step. Electrochemical characterization displayed a possible double-layer effect ruling the system, with higher current intensities (good capacitance contribution) observed in the presence of the LbL films due to conductive paths formed by the graphene nanoplatelets in the layered LbL film structure, without noticeable effects from the wrapping materials (chitosan or PSS). Results presented here are a promising step for future studies in electron transfer mechanisms between enzymes and electrodes.

Acknowledgements

Authors are grateful to BE-Basic Foundation, FAPESP (Proc. 14/03691-7), CNPq, CAPES, Grupo de Polímeros Prof. Berhnard Gross (IFSC, USP) for the FTIR measurements and also to Dr. David Sotero dos Santos Jr (OSHTECH, Canada) for kindly donating chitosan.

References

1. Soldano C, Mahmood A, Dujardin E (2010) Production, properties and potential of graphene. Carbon 48: 2127-2150.
2. Hummers WS, Offeman RE (1958) Preparation of Graphitic Oxide. J Am Chem Soc 80: 1339.

3. Zhang S, Shao Y, Liao H, Engelhard MH, Yin G, et al. (2011) Polyelectrolyte-induced reduction of exfoliated graphite oxide: a facile route to synthesis of soluble graphene nanosheets. ACS Nano 5: 1785-1791.
4. Loh KP, Bao Q, Eda G, Chhowalla M (2010) Graphene oxide as a chemically tunable platform for optical applications. Nat Chem 2: 1015-1024.
5. Zhu Y, Murali S, Cai W, Li X, Suk JW, et al. (2010) Graphene and graphene oxide: synthesis, properties, and applications. Adv Mater 22: 3906-3924.
6. Silva JS, De Barros A, Constantino CJ, Simões FR, Ferreira M (2014) Layer-by-layer films based on carbon nanotubes and polyaniline for detecting 2-chlorophenol. J Nanosci Nanotechnol 14: 6586-6592.
7. Tian M, Hu X, Qu L, Zhu S, Sun Y, et al. (2016) Versatile and ductile cotton fabric achieved via layer-by-layer self-assembly by consecutive adsorption of graphene doped PEDOT: PSS and chitosan. Carbon 96 : 1166-1174.
8. Decher G (1997) Fuzzy Nanoassemblies: Toward Layered Polymeric Multicomposites. Science 277: 1232-1237.
9. Richardson JJ, Björnmalm M, Caruso F (2015) Multilayer assembly. Technology-driven layer-by-layer assembly of nanofilms. Science 348: aaa2491.
10. Lutkenhaus JL, Hammond PT (2007) Electrochemically enabled polyelectrolyte multilayer devices: from fuel cells to sensors. Soft Matter 3: 804-816.
11. Graça JS, de Oliveira RF, de Moraes ML, Ferreira M (2014) Amperometric glucose biosensor based on layer-by-layer films of microperoxidase-11 and liposome-encapsulated glucose oxidase. Bioelectrochemistry 96: 37-42.
12. Bough WA, Salter WL, Wu ACM, Perkinns BE (1978) Influence of manufacturing variables on the characteristics and effectiveness of chitosan products. I. Chemical composition, viscosity, and molecular-weight distribution of chitosan products. Biotechnology and Bioengineering 20: 1931-1943.
13. Kovtyukhova NI, Ollivier PJ, Martin BR, Mallouk TE, Chizhik SA, et al. (1999) Layer-by-Layer Assembly of Ultrathin Composite Films from Micron-Sized Graphite Oxide Sheets and Polycations. Chem Mater 11: 771-778.
14. Khanra P, Kuilaa T, Kimb NH, Baea SH, Yua D, et al. (2012) Simultaneous bio-functionalization and reduction of graphene oxide by baker's yeast. Chem Eng J 183: 526-533.
15. Villar-Rodil S, Paredes JI, Martínez-Alonsoa A, Tascóna JMD (2009) Preparation of graphene dispersions and graphene-polymer composites in organic media. J Mater Chem 19: 3591-3593.
16. Jiang G, Baba A, Advincula R (2007) Nanopatterning and fabrication of memory devices from layer-by-layer poly(3,4-ethylenedioxythiophene)-poly(styrene sulfonate) ultrathin films. Langmuir 23: 817-825.
17. Kumirska J, Czerwicka M, Kaczyński Z, Bychowska A, Brzozowski K, et al. (2010) Application of spectroscopic methods for structural analysis of chitin and chitosan. Mar Drugs 8: 1567-1636.
18. Volpati D, Machado AD ,Olivati CA, Alves N, Curvelo AAS, et al. (2011) Physical Vapor Deposited Thin Films of Lignins Extracted from Sugar Cane Bagasse: Morphology, Electrical Properties, and Sensing Applications. Biomacromolecules 12: 3223-3231.
19. Wu N, She X, Yang D, Wu X,Su F, et al. (2012) Synthesis of network reduced graphene oxide in polystyrene matrix by a two-step reduction method for superior conductivity of the composite. J Mater Chem 22: 17254-17261.
20. Stankovich S, Piner RD, Chen X, Wu N, Nguyen ST, et al. (2006) Stable aqueous dispersions of graphitic nanoplatelets via the reduction of exfoliated graphite oxide in the presence of poly(sodium 4-styrenesulfonate). J Mater Chem 16: 155-158.
21. Espinosa-Andrews H, Sandoval-Castilla O, Vázquez-Torres H, Vernon-Carter EJ, Lobato-Calleros C (2010) Determination of the gum Arabic-chitosan interactions by Fourier Transform Infrared Spectroscopy and characterization of the microstructure and rheological features of their coacervates. Carbohydrate. Polymers 79: 541-546.
22. Fernandes LL, Resende CX, Tavares DS, Soares GA, Castro LO, et al. (2011) Cytocompatibility of chitosan and collagen-chitosan scaffolds for tissue engineering. Polímeros 21: 1-6.
23. Lu J, Do I, Fukushima H, Lee I, Drzal LT (2010) Stable Aqueous Suspension and Self-Assembly of Graphite Nanoplatelets Coated with Various Polyelectrolytes. J Nanomater 2010: 186486.
24. Cardenas G, Miranda SP (2004) Ftir and TGA studies of chitosan composite films. J Chil Chem Soc 49: 291-295.
25. Pullini D, Siong V, Tamvakos D, Ortega BL, Sgroi MF, et al. (2015) Enhancing the capacitance and active surface utilization of supercapacitor electrode by graphene nanoplatelets. Compos Sci Technol 112: 16-21.

Citation: Almeida TP, Miyazaki CM, Volpati D, Silva TA, Braunger ML, et al. (2016) Ultra-Thin Films of Reduced Graphene Oxide (RGO) Nanoplatelets Functionalized with Different Organic Materials. J Bioprocess Biotech 6: 272. doi:10.4172/2155-9821.1000272